

Original articles

Research article

<https://doi.org/10.17308/kcmf.2022.24/9051>**Preparation and characterisation of cobalt and cobalt-zinc ferrites for magnetorheological materials**Yu. S. Haiduk¹✉, E. V. Korobko², D. A. Kotsikau¹, I. A. Svito¹, A. E. Usenka¹, V. V. Pankov¹¹Belarusian State University,
4 Nezavisimosty pr., Minsk 220030, Belarus²A. V. Luikov Heat and Mass Transfer Institute of NAS of Belarus,
15 P. Brovki ul., Minsk 220072, Belarus**Abstract**

The aim of this study was to study the structure, morphology, magnetic, and magnetorheological properties of cobalt and cobalt-zinc ferrite powders to be used as a functional component of magnetorheological fluids.

Ferrites of cobalt CoFe_2O_4 and cobalt-zinc $\text{Co}_{0.65}\text{Zn}_{0.35}\text{Fe}_2\text{O}_4$ were obtained by combined hydrolysis of inorganic metal salt in aqueous solutions followed by thermal treatment of the precipitates. The ferrites were studied by means of X-ray phase analysis, scanning electron microscopy, IR spectroscopy, and magnetometry.

The synthesised ferrites are polydispersed powders with the size of primary particles of 300–400 nm and the size of the coherent scattering regions of 22–33 nm. They demonstrate a high shear stress in magnetorheological suspensions, which is 2.5 times higher than that of the nanosized particles. High-temperature annealing results in a significant increase in the specific magnetisation of the powders, as well as the shear stress in suspensions prepared on their basis. Doping cobalt ferrite with zinc leads to an increase in the specific magnetisation and rheological characteristics.

The studied materials have a high shear stress in suspensions (~ 2.5 kPa at 650 mT) and can be used as functional fillers for magnetorheological materials.

Keywords: Cobalt ferrite, Cobalt-zinc ferrite, Magnetorheological materials

For citation: Haiduk Yu. S., Korobko E. V., Kotsikau D. A., Svito I. A., Usenka A. E., Pankov V.V. Preparation and characterisation of cobalt and cobalt-zinc ferrites for magnetorheological materials. *Kondensirovannyye sredy i mezhfaznye granitsy = Condensed Matter and Interphases*. 2022;24(1): 19–28. <https://doi.org/10.17308/kcmf.2022.24/9051>

Для цитирования: Гайдук Ю. С., Коробко Е. В., Котиков Д. А., Свито И. А., Усенко А. Е., Паньков В. В. Получение и характеристика ферритов кобальта и кобальта-цинка для магнитореологических материалов *Конденсированные среды и межфазные границы*. 2022;24(1): 19–28. <https://doi.org/10.17308/kcmf.2022.24/9051>

✉ Yulyan S. Haiduk, e-mail: j_hajduk@bk.ru

© Haiduk Yu. S., Korobko E. V., Kotsikau D. A., Svito I. A., Usenka A. E., Pankov V. V., 2022



1. Introduction

Magnetic fluids (MF) and magnetorheological fluids (MRF) belong to the category of magnetically controllable materials. They differ in the degree of the magnetorheological effect, which is much stronger in MRFs than in MFs. MFs usually contain nanosized magnetic particles, whose concentration in the composition does not exceed a few vol%. The concentration of magnetic particles in MRFs can reach up to 50 vol%, and their size usually exceeds 0.1 μm [1]. MRFs are used as an active medium for damping devices designed for the protection of vehicles, industrial equipment, buildings, and structures from vibrations and other mechanical influences, as well as for shaft hermitization, production of prostheses, and production of recoil devices and return systems for artillery, etc. [2].

The most common way to gain the magnetorheological response of a suspension is to increase the magnetisation of micro- and nanosized magnetic particles reducing the coercivity, as well as to obtain anisometric particles (for instance, needle-like particles). In order to do this, it is necessary to enhance the existing methods for synthesising magnetic materials. A promising solution is to combine micro- or nanoparticles rather than to use them separately. It is known that micron particles demonstrate stronger magnetorheological effect, and their combination with nanoparticles stabilises the suspension preventing or slowing down the aggregation and sedimentation processes. A combined effect of several factors (the morphology of the particles, their magnetisation, the coercive force, and the mass fraction in the suspension) can lead to a synergistic effect, which in turn results in an emergent viscosity effect.

Cobalt and cobalt-zinc ferrites synthesised by means of chemical coprecipitation [3–6], the sol-gel method [7], electrostatic spraying [8] and other methods are being actively studied as promising ferrimagnetic materials. Zinc ferrite has a cubic spinel lattice with normal distribution of cations in the spinel sublattices, while cobalt ferrite has a reverse structure. Structural deviations result in a nonequilibrium distribution of cations in the lattice and cause a change in the magnetic properties [9–11]. In addition, changing the distribution of the cations in the ferrite lattice

by forming solid solutions between certain ferrite compositions, we can alter the magnetic properties of the material to a certain degree. Thus, the introduction of a non-magnetic Zn^{2+} ion to the lattice of cobalt ferrite with a strong preference for tetrahedral positions will cause the migration of Fe^{3+} ions into the octahedral positions, leading to an increase in the magnetic moment.

In our earlier study [12], we developed a technique that allows controlling the magnetic properties of cobalt-zinc ferrite by substituting for cobalt ions in the structure of Co-Zn spinel with a non-magnetic double charge cation, namely zinc. We found that an increase in the magnetisation and a decrease in the coercivity occurs until the concentration of zinc reaches $x = 0.35$ ($\text{Co}_{0.65}\text{Zn}_{0.35}\text{Fe}_2\text{O}_4$). The ferrites obtained by spray-drying followed by annealing in the inert component matrix (NaCl) consisted of particles that are uniform in size (~ 50 nm), some of them being in a superparamagnetic state. The powder had specific magnetisation of about ~ 45 $\text{A}\cdot\text{m}^2\text{kg}^{-1}$ and demonstrated a shear stress of ~ 1 kPa in a suspension based on industrial oil, with the magnetic field induction being 600 mT [12].

The aim of this study was to study the structure, morphology, magnetic, and magnetorheological properties of cobalt and cobalt-zinc ferrite powders to be used as a functional components of magnetorheological materials, namely magnetorheological fluids. To increase the average size of the particles, their specific magnetisation, and, as a result, the shear stress in ferrite suspensions, we used the method of chemical precipitation from aqueous solutions followed by high-temperature treatment of the precipitates in air.

2. Experimental

The CoFe_2O_4 ferrite powder was obtained from solutions of the metal salts followed by high-temperature annealing. Samples of $\text{CoSO}_4\cdot 7\text{H}_2\text{O}$ weighing 36.54 g and $\text{Fe}(\text{NO}_3)_3\cdot 9\text{H}_2\text{O}$ weighing 52.54 g were dissolved in 1 l of distilled water. An ammonia solution was poured into the resulting salt solution with vigorous stirring. The pH level of the resulting suspension was monitored (pH = 11.0). The suspension was heated to 90 °C. The precipitate was washed by magnetic

decantation, after which it was heat treated at 740 °C for 8 h in air and ground in an agate mortar.

To obtain $\text{Co}_{0.65}\text{Zn}_{0.35}\text{Fe}_2\text{O}_4$ samples, powders of $\text{CoSO}_4 \cdot 7\text{H}_2\text{O}$ (16.25 g), ZnCl_2 (4.26 g), and $\text{Fe}(\text{NO}_3)_3$ (49.81 g) were dissolved in 1.5 l of distilled water. The solution was stirred with magnetic stirrer for 5 min to reach complete homogenisation. An ammonia solution was poured into the resulting salt solution under vigorous stirring and the pH level of the formed suspension was monitored using indicator paper (pH = 11.0). The suspension was heated to 90 °C. The precipitate was washed by magnetic decantation [12], after which it was heat treated at 740 °C for 8 h and ground in an agate mortar.

X-ray studies were performed using a DRON-3 diffractometer (CoK_α -radiation, $\lambda = 0.1790$ nm) within an angle range of $2\theta = 6\text{--}90^\circ$. The sizes of coherent scattering regions (CSR) were determined by the broadening of diffraction reflections (Scherrer method).

The radiodensity was calculated using the formula:

$$d_x = \frac{8M}{a^3 N_A}, \quad (1)$$

where M is formal molecular weight; a is the lattice parameter, and Å ; N_A is Avogadro number.

The degree of crystallinity of the samples was determined using the ratio:

$$\left(1 - \frac{I_{\text{background}}}{I_{311}}\right) \times 100\%, \quad (2)$$

where I_{311} is the intensity of the reflex of the spinel, corresponding to the crystallographic direction 311; $I_{\text{background}}$ is the intensity of the background line of the x-ray diffraction pattern.

Dislocation density δ (number of lines per 1 m^2) was calculated using the formula:

$$\delta = \frac{1}{D^2}. \quad (3)$$

IR-spectra were recorded using an AVATAR FTIR-330 spectrometer (Thermo Nicolet) in the wavenumber region (ν) 400–700 cm^{-1} with a resolution of ± 1 cm^{-1} . The spectra were registered in adiffuse scattering mode using the Smart Diffuse Reflectance accessory.

The surface structure of polycrystalline and film samples was studied by means of

scanning electron microscopy using a LEO 1420. Simultaneously, the ratio of the concentration of metal atoms in ferrite powders and the features of their distribution on the surface of the particles were determined by energy dispersive X-ray spectroscopy (EDX-analysis).

The magnetic characteristics were studied using a Cryogen Free Measurement System from Cryogenic Ltd, where hysteresis loops were recorded at temperatures of 10 and 300 K and magnetic field induction $B_{\text{max}} = 8$ T. The weight of the samples, not including the capsule, was 0.04134 g for CoFe_2O_4 and 0.0685 g for $\text{Co}_{0.65}\text{Zn}_{0.35}\text{Fe}_2\text{O}_4$.

The dependence of the shear stress (τ) of the suspensions on the magnetic induction of the applied magnetic field was measured using a Physics MCR 301 AntonPaar rotational viscometer in constant shear rate mode (Mobil 22 binder, shear rate $\dot{\gamma} = 200$ s^{-1} , $T = 20^\circ$ C). Powder suspensions in the binder were prepared using a UZDM-2 ultrasonic disperser with a frequency of 44 kHz.

3. Results and discussion

Fig. 1 demonstrates the XRD spectra of the CoFe_2O_4 and $\text{Co}_{0.65}\text{Zn}_{0.35}\text{Fe}_2\text{O}_4$ ferrites, obtained by means of coprecipitation followed by thermal treatment in air (740 °C, 8 h), and the XRD spectrum of the $\text{Co}_{0.65}\text{Zn}_{0.35}\text{Fe}_2\text{O}_4$ ferrite, obtained in [12] by spray-drying followed by thermal treatment in air (740 °C, 8 h) for comparison.

By analysing the XRD spectra we can say that in all the three cases the formation of the spinel ferrite structure (space group $Fd\bar{3}m$) is completed under the set thermal treatment conditions. The diffraction peaks demonstrate high intensity and slight broadening, which indicates the formation of a highly ordered crystal lattice. The peaks positions and their relative intensities indicate the presence of a single phase with a spinel structure. The structural parameters of the crystal lattice are given in Table 1.

The size of the coherent scattering regions corresponding to the physical sizes of crystallites was 36 and 31 nm for CoFe_2O_4 and $\text{Co}_{0.65}\text{Zn}_{0.35}\text{Fe}_2\text{O}_4$ obtained by coprecipitation, which is significantly greater than that of the sample obtained by spray-drying (20 nm). This is accounted for by the fact that the annealing of ferrite in the

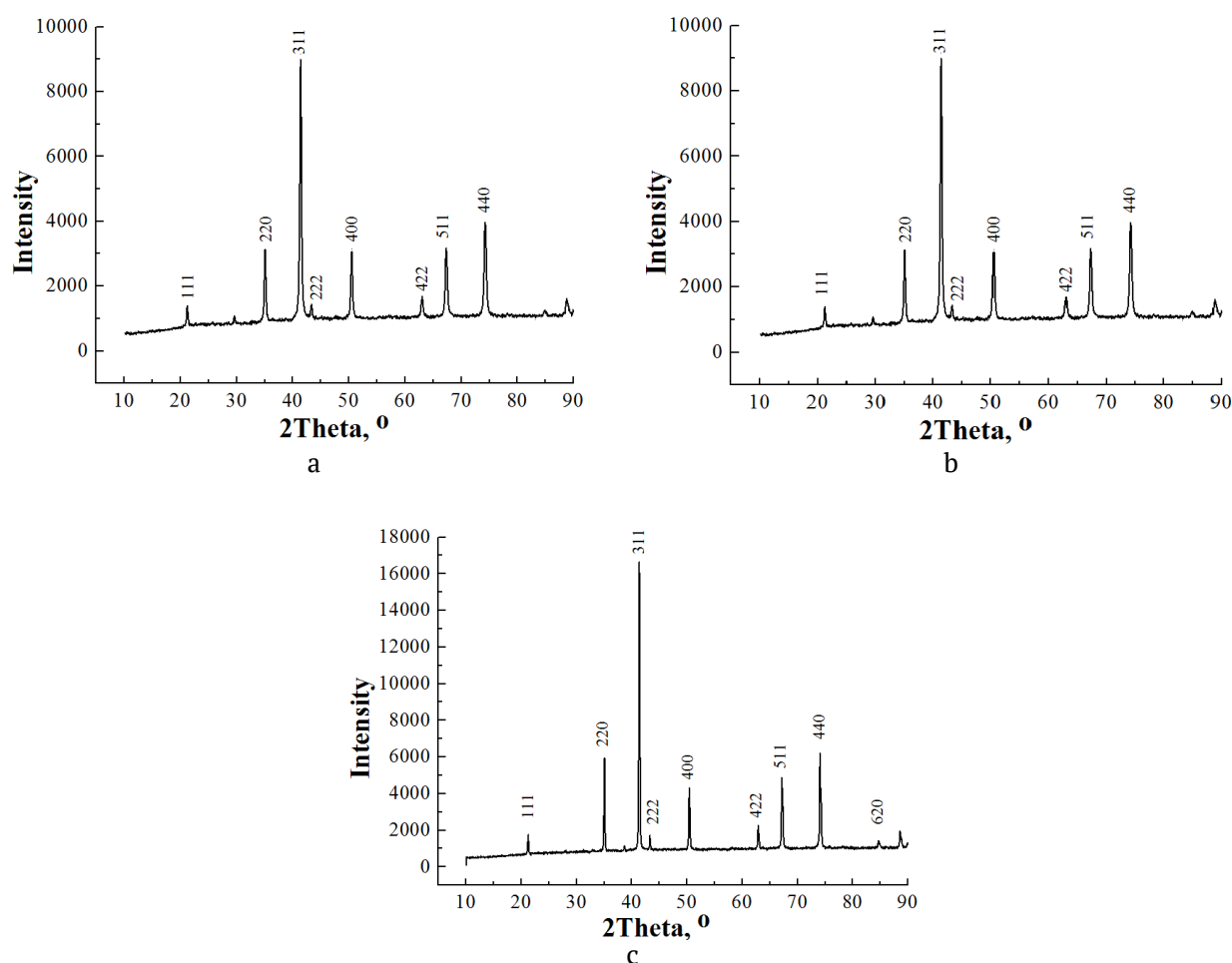


Fig. 1. XRD spectra: a) $\text{Co}_{0.65}\text{Zn}_{0.35}\text{Fe}_2\text{O}_4$ (spray-drying); b) CoFe_2O_4 (coprecipitation), c) $\text{Co}_{0.65}\text{Zn}_{0.35}\text{Fe}_2\text{O}_4$ (coprecipitation)

Table 1. The structural parameters of the crystal lattice: lattice constant a , unit cell volume V , size of the CSR D , dislocation density δ , radiodensity d_x , degree of crystallinity d_c for $\text{Co}_{0.65}\text{Zn}_{0.35}\text{Fe}_2\text{O}_4$ powders (spray-drying) (1), CoFe_2O_4 (coprecipitation) (2), $\text{Co}_{0.65}\text{Zn}_{0.35}\text{Fe}_2\text{O}_4$ (coprecipitation) (3)

Sample	$a, \text{\AA}$	V, nm^3	D, nm	$\delta \times 10^2 \text{nm}^{-2}$	$d_x, \text{g/cm}^3$	$d_c, \%$
1	8,3998	592,626	20	0,2500	5,310	85
2	8,3898	590,554	22	0,2066	5,279	88
3	8,4037	593,488	33	0,0918	5,293	94

inert sodium chloride medium hinders the growth of crystallites. The samples obtained by coprecipitation also demonstrate higher crystallinity and lower dislocation density.

Fig. 2. shows fragments of SEM micrographs of the studied CoFe_2O_4 and $\text{Co}_{0.65}\text{Zn}_{0.35}\text{Fe}_2\text{O}_4$ powders, which demonstrate a high degree of agglomeration of the particles. Agglomerates larger than $1 \mu\text{m}$ appear either due to the surface properties of the particles, or due to the fact that the thermal treatment conditions induced the

first stage of the sintering accompanied by the formation of small bridges between the particles. The primary particles have the size of $300 - 400 \text{ nm}$ and a specific shape with pronounced facets. $\text{Co}_{0.65}\text{Zn}_{0.35}\text{Fe}_2\text{O}_4$ particles are more crystallized because the temperature of the synthesis and sintering of zinc ferrite is much lower than that of cobalt ferrite.

A comparison of the size of crystallites (coherent scattering regions), calculated by the diffractometry method (Table 1), and the size of

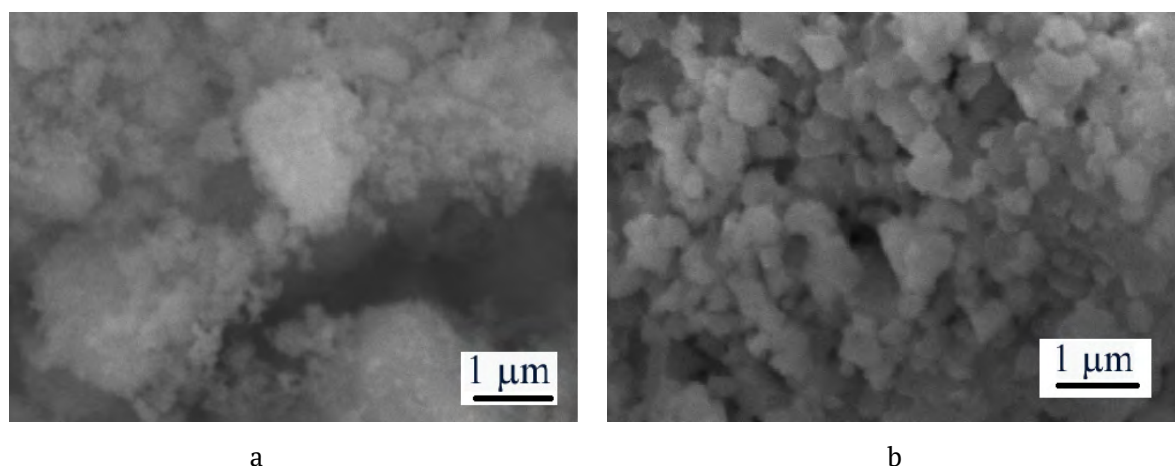


Fig. 2. SEM micrographs: a) CoFe_2O_4 (coprecipitation); b) $\text{Co}_{0.65}\text{Zn}_{0.35}\text{Fe}_2\text{O}_4$ (coprecipitation)

the particles demonstrated that after annealing at $740\ \text{°C}$ some particles include several crystallites and are multidomain. It is known that the critical size for the transition of a single-domain particle to a multidomain at $300\ \text{K}$ is around $40\ \text{nm}$ (for cobalt ferrite, for instance) [13]. In the region of transition to the ferromagnetic state, following the growth of the particles crystallites spontaneously break up into several domains in order to reduce high magnetisation energy of a single-domain particle.

Fig. 3 shows the IR absorption spectra of the CoFe_2O_4 and $\text{Co}_{0.65}\text{Zn}_{0.35}\text{Fe}_2\text{O}_4$ powders.

In the region of characteristic frequencies both CoFe_2O_4 and $\text{Co}_{0.65}\text{Zn}_{0.35}\text{Fe}_2\text{O}_4$ spectra demonstrate pronounced combined vibrational bands of $\text{Me}-\text{O}$ (at 414 and $567\ \text{cm}^{-1}$). The band at $414\ \text{cm}^{-1}$ usually refers to the octahedral

vibrations of the metal $\text{Me}_{\text{octa}} \leftrightarrow \text{O}$, and the band at $567\ \text{cm}^{-1}$ corresponds to the internal stretching vibrations of the metal in the site $\text{Me}_{\text{tetra}} \leftrightarrow \text{O}$ [5]. The said absorption bands are also observed in the spectrum of $\text{Co}_{0.65}\text{Zn}_{0.35}\text{Fe}_2\text{O}_4$ obtained by spray-drying [12]. All the bands have a high degree of resolution, which may reflect a high ordering of the crystal structure.

A wide absorption band at $1600\ \text{cm}^{-1}$ [12], corresponding to vibrations of adsorbed water [11], is much less prominent in the CoFe_2O_4 sample (Fig. 3a) and practically absent in the $\text{Co}_{0.65}\text{Zn}_{0.35}\text{Fe}_2\text{O}_4$ sample (Fig. 3b). The spectrum of $\text{Co}_{0.65}\text{Zn}_{0.35}\text{Fe}_2\text{O}_4$ obtained by spray-drying also demonstrated absorption at $2100\text{--}2300\ \text{cm}^{-1}$, $1500\text{--}1600\ \text{cm}^{-1}$, and near $1000\ \text{cm}^{-1}$ (presumably explained by the absorption of CO_2 molecules and NO_3^- ions). The corresponding absorption

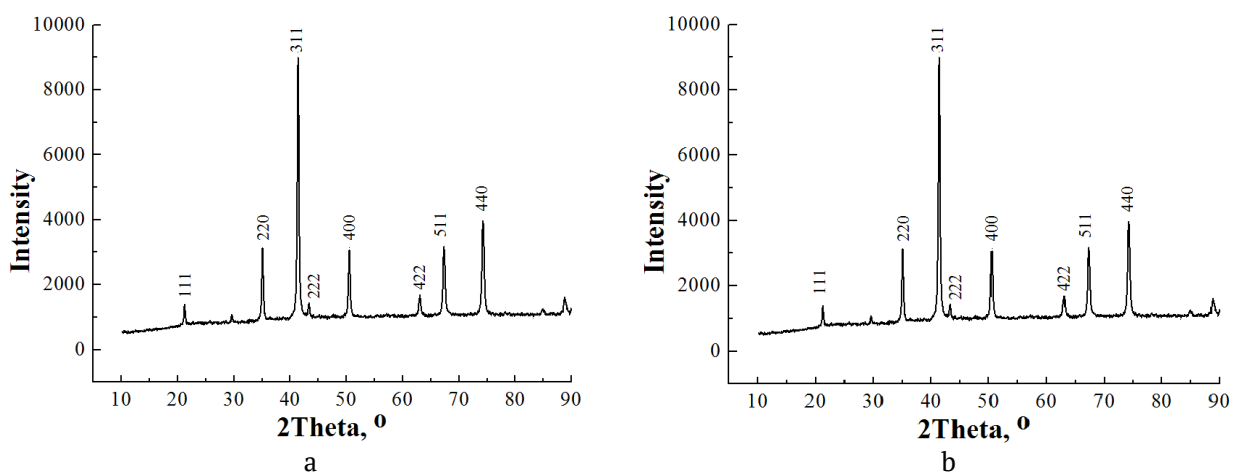


Fig. 3. IR absorption spectrum: a) CoFe_2O_4 ; b) $\text{Co}_{0.65}\text{Zn}_{0.35}\text{Fe}_2\text{O}_4$

bands are much less prominent in the spectrum of CoFe_2O_4 (Fig. 3a) and absent in the spectrum of the $\text{Co}_{0.65}\text{Zn}_{0.35}\text{Fe}_2\text{O}_4$ sample obtained by coprecipitation (Fig. 3b).

Fig. 5 shows the change in magnetisation for CoFe_2O_4 and $\text{Co}_{0.65}\text{Zn}_{0.35}\text{Fe}_2\text{O}_4$ obtained by coprecipitation depending on the magnetic field induction. Both powders exhibited ferrimagnetic behaviour. The specific magnetisation of the $\text{Co}_{0.65}\text{Zn}_{0.35}\text{Fe}_2\text{O}_4$ powder obtained in this study exceeds the specific magnetisation of cobalt-zinc ferrites of the same composition obtained using other methods, namely the sol-gel method ($60\div 80 \text{ A}\cdot\text{m}^2 \text{ kg}^{-1}$) [14, 15] and coprecipitation from aqueous solutions of inorganic salts ($40\div 70 \text{ A}\cdot\text{m}^2 \text{ kg}^{-1}$) [16], ($60 \div 90 \text{ A}\cdot\text{m}^2 \text{ kg}^{-1}$) [17].

In our earlier article we demonstrated that with an increase in the zinc content in the cobalt-zinc ferrite, an increase in the saturation magnetisation was noted. Thus, for the $\text{Co}_{0.65}\text{Zn}_{0.35}\text{Fe}_2\text{O}_4$ powder the magnetisation was $M_s = 42.6 \text{ A}\cdot\text{m}^2 \text{ kg}^{-1}$, and for the CoFe_2O_4 powder it was $M_s = 25.0\text{--}26.0 \text{ A}\cdot\text{m}^2 \text{ kg}^{-1}$. When the concentration of Zn^{2+} ions increased from 0 to 0.35, the total magnetisation ($M_{\text{oct.}}M_{\text{tet.}}$) for $\text{Co}_{1-x}\text{Zn}_x\text{Fe}_2\text{O}_4$ also increased due to the displacement of iron ions to the octahedral positions of the spinel by the zinc ions. The increase in the magnetisation of the ferrite is accompanied by an increase in interlattice AB superexchange interactions [12]. When the number of substituting Zn^{2+} ions is large enough ($x > 0.35$), the antiferromagnetic interaction of Fe^{3+} ions located in neighbouring positions in the octahedral sublattice begins. Therefore, the BB interaction leads to a decrease in the total magnetic moment [12].

It was also established earlier, that doping cobalt ferrite with zinc ions results in a decrease in the coercive force for the same particle sizes

[7, 12]. This is explained by the reduction of the magnetic anisotropy of doped powders. Particles of the critical size, i.e. particles on the border of the ferromagnetic state, have the highest coercive force. For cobalt ferrite, the size of such particles is $\sim 40 \text{ nm}$. With the further growth of the particles the coercive force decreases. This dependence can be accounted for by the domain structure, the critical size of the particles, and the degree of the anisotropy of the surface and intercrystalline boundaries. The coercivity of 0.27 kOe obtained at 300 K is much lower than the theoretically calculated coercivity of cobalt (5.3 kOe) [13], which indicates the ferrimagnetic state of the particles.

The magnetic parameters of the powders calculated based on the magnetic hysteresis loops of CoFe_2O_4 and $\text{Co}_{0.65}\text{Zn}_{0.35}\text{Fe}_2\text{O}_4$ are given in Table 2.

The shape of the magnetisation curves shown in Fig. 4 is similar to the shape described in the literature and is characterized by their significant rectangularity [18]. Table 2 shows that the value of M_s slightly decreases with the growth of temperature, while the adjusted residual magnetisation M_r/M_s and the coercivity H_c decrease significantly. This happens due to the influence of thermal fluctuations of the magnetisation of individual particles [18–20]. For CoFe_2O_4 $M_r/M_s = 0.83$ at low temperatures, which, according to the Stoner-Wohlfarth model, indicates the presence of cubic anisotropy, while for $\text{Co}_{0.65}\text{Zn}_{0.35}\text{Fe}_2\text{O}_4$ it is not observed ($M_r/M_s < 0.5$) [12]. The uncharacteristic kinks on the magnetisation curves (Fig. 4a) can result from the interaction between the hard and soft anisotropy regimes, the polydispersity of the powder, the shape of the particles, and their interaction [12].

Table 2 demonstrates that the coercivity of the zinc-containing ferrite is much lower than

Table 2. The parameters of the magnetisation curves of CoFe_2O_4 and $\text{Co}_{0.65}\text{Zn}_{0.35}\text{Fe}_2\text{O}_4$ powders (saturation magnetisation M_s , adjusted remanent magnetisation M_r/M_s , coercivity H_c)

T, K	CoFe_2O_4			$\text{Co}_{0.65}\text{Zn}_{0.35}\text{Fe}_2\text{O}_4$		
	M_s , $\text{A}\cdot\text{m}^2 \text{ kg}^{-1}$	M_r/M_s	H_c , kOe	M_s , $\text{A}\cdot\text{m}^2 \text{ kg}^{-1}$	M_r/M_s	H_c , kOe
10	83.3	0.77	12.5	123.6	0.44	1.35
100	83.5	0.74	8.0	122.4	0.39	1.1
200	80.7	0.60	3.1	112.5	0.23	0.5
300	73.2	0.37	0.27	97.9	0.12	0.1

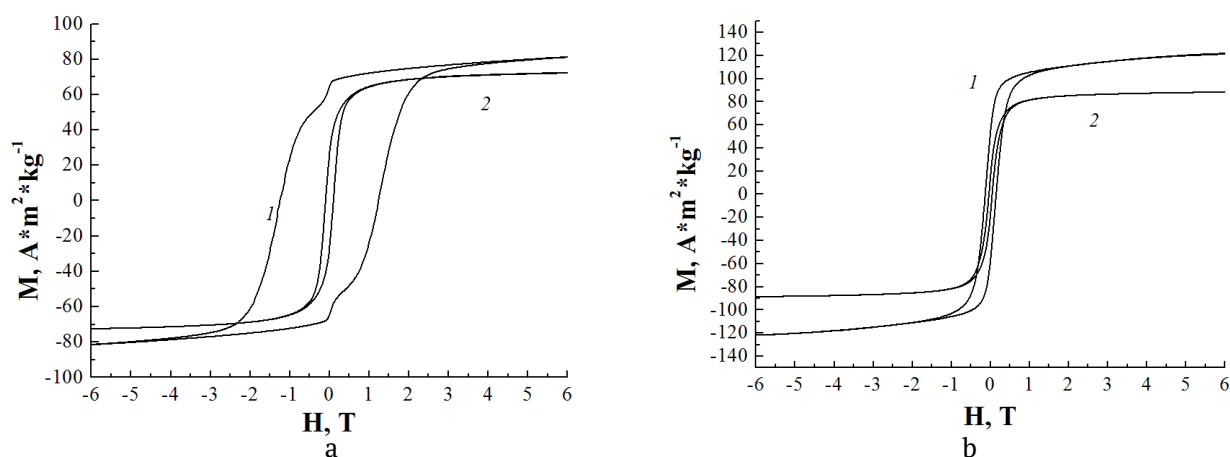


Fig. 4. Curves of the dependence of the magnetisation on the magnetic field strength at different temperatures 1 – 10 K, 2 – 300 K: a) CoFe_2O_4 ; b) $\text{Co}_{0.65}\text{Zn}_{0.35}\text{Fe}_2\text{O}_4$

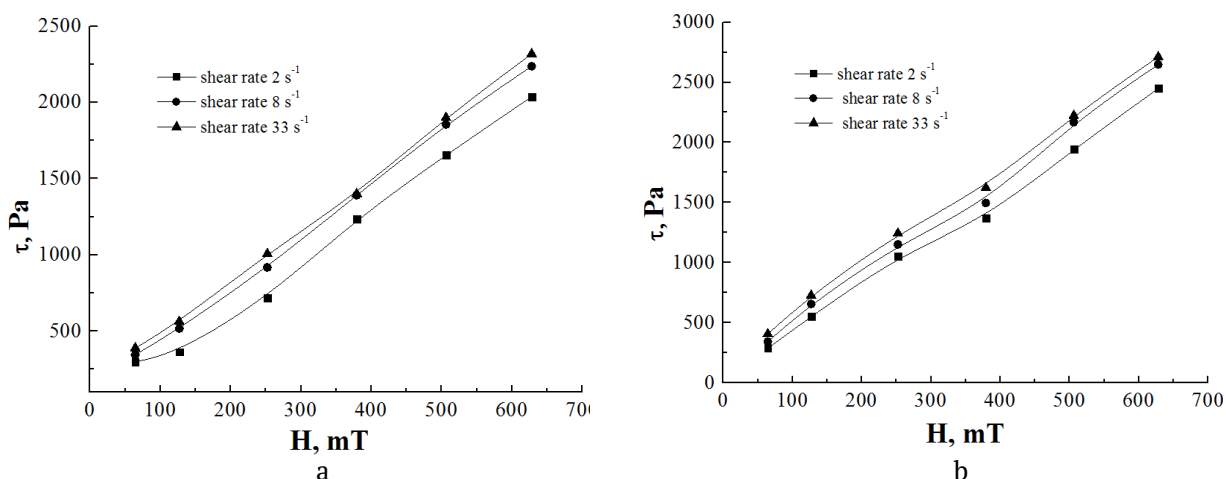


Fig. 5. Dependence of the shear stress of MRF containing 20 wt% of ferrite powder in Mobil 22 on the magnetic field induction at shear rates of 2, 8, and 33 s^{-1} : a) CoFe_2O_4 ; b) $\text{Co}_{0.65}\text{Zn}_{0.35}\text{Fe}_2\text{O}_4$

that of CoFe_2O_4 . This is associated primarily with the characteristic constant of the material anisotropy and the introduction of zinc ions into the ferrite structure [12]. The presence of inhomogeneities, impurities, and crystal lattice defects preventing the remagnetisation of the sample, also increase H_c . These factors are associated with the method of synthesising the sample. $\text{Co}_{0.65}\text{Zn}_{0.35}\text{Fe}_2\text{O}_4$ powder obtained in this study has $H_c = 0.1$ kOe at 300 K, while the coercivity of the sample obtained by spray-drying in sodium chloride medium was 0.4 kOe [12]. With regard to MRFs, it is advisable to use ferrites with lower coercivity in order to increase the magneto-control of the composition.

The comparison of M_s for $\text{Co}_{0.65}\text{Zn}_{0.35}\text{Fe}_2\text{O}_4$ obtained by spray-drying followed by annealing

in the NaCl medium in [12] and for the sample obtained by coprecipitation followed by annealing in air under the same conditions (Table 2) demonstrated a significant increase in the specific magnetisation for the coprecipitation method. The high-temperature annealing of the $\text{Co}_{0.65}\text{Zn}_{0.35}\text{Fe}_2\text{O}_4$ powder in air results in the formation of larger particles with a higher degree of crystallinity as compared to the annealing in the NaCl matrix. The surface layer of the particles with random spin orientation has much less effect on the magnetic properties of the particles than in the former case, which is why the specific magnetisation is much higher. Therefore, the suggested annealing conditions proved to be optimal for obtaining high magnetisation of $\text{Co}_{0.65}\text{Zn}_{0.35}\text{Fe}_2\text{O}_4$. In this case, we minimised the

negative effect of the non-magnetic surface layer of the particles, while the particles retained their individuality at the nano scale without sintering.

The CoFe_2O_4 and $\text{Co}_{0.65}\text{Zn}_{0.35}\text{Fe}_2\text{O}_4$ powders obtained by coprecipitation have high oil absorption and form fairly stable suspensions in the industrial Mobil 22 oil. This makes it possible to use them as functional fillers for magnetorheological materials, including magnetorheological suspensions based on carbonyl iron in synthetic oil. In the latter case, the ferrite additives would perform the modifying and stabilising functions. Fig. 5 shows the dependences of the shear stress of an MRF on the magnetic field induction at different shear rates for the MRF containing 20 wt% of ferrite powder in the industrial Mobil 22 oil.

A high value of shear stress (over 2500 Pa) at 650 mT indicated that the studied powders can be considered promising materials for the above listed applications. It should be noted that the previously studied $\text{Co}_{0.65}\text{Zn}_{0.35}\text{Fe}_2\text{O}_4$ powder obtained by spray-drying at 650 mT demonstrated the shear stress of ~ 1000 Pa [12]. Such a significant increase in the shear stress for the obtained samples is explained by the conditions of the synthesis, namely the high-temperature annealing. Comparing the $\text{Co}_{0.65}\text{Zn}_{0.35}\text{Fe}_2\text{O}_4$ powders obtained by spray-drying [12] and coprecipitation, we can see that besides the increase in the particle size and the degree of crystallinity (from 85 to 97 %) the annealing results in a change in the shape of the particles from spherical to faceted. Such morphological changes influence the rheological behaviour of the powders in the suspension resulting in an increase in the shear stress. At the same time, the density and the oil absorption of the particles can also increase.

4. Conclusions

In this paper we proposed a new technique for synthesising cobalt and cobalt-zinc ferrites based on the method of coprecipitation from aqueous solutions of the corresponding salts. The technique involves high-temperature annealing of the precipitates in air which results in highly crystalline polydispersed powders with high specific saturation magnetisation ($97.9 \text{ A}\cdot\text{m}^2\cdot\text{kg}^{-1}$ at 300 K).

The synthesised ferrites are polydispersed powders with the size of primary particles of 300–400 nm and the size of the coherent scattering regions of 30–35 nm. They demonstrate high shear stress in magnetorheological suspensions, which is 2.5 times higher than that of the nanosized particles.

In our study, we also obtained suspensions of the ferrite powders with the industrial Mobil 22 oil (20 wt%) for the analysis of the dependences of the shear stress on the magnetic field induction. The high shear stress (2.5 kPa) with a relatively low magnetic field induction (from 600 mT and above) allowed us to consider the obtained materials as being promising for use as functional fillers for magnetorheological materials, including magnetorheological suspensions of damping devices.

Author contributions

Haiduk Yu. S. – writing the article, synthesising the materials, conducting research, interpreting the results. Korobko E. B. – conducting research (magnetorheological measurements), interpreting the results, scientific editing. Kotsikau D. A. – conducting research (IR spectroscopy), scientific editing. Svito I. A. – conducting research (magnetic measurements), interpreting the results. Usenko A. E. – scientific leadership, interpreting the results. Pankov V. V. – scientific leadership, research concept, interpreting the results, final conclusions.

Conflict of interests

The authors declare that they have no known competing financial interests or personal relationships that could have influenced the work reported in this paper.

References

1. Vekas L. Ferrofluids and magnetorheological fluids. *Advances in Science and Technology*. 2008;54(1):127–136. <https://doi.org/10.4028/www.scientific.net/AST.54.127>
2. Belyaev E. S., Ermolaev A. I., Titov E. Yu., Tumakov S. F. *Magnetorheological fluids: technologies of creation and application*. N. Novgorod; Nizhegorod. state tech. un-t them. R. E. Alekseeva. 2017. 94 p. (In Russ.). <http://www.vntr.ru/lib/vntr18-VOL7.pdf>
3. Mayekar J., Dhar V., Radha S. Synthesis, Characterization and magnetic study of zinc ferrite nanoparticles. *International Journal of Innovative*

- Research in Science, Engineering and Technology*. 2016;5(5): 83678371. <https://doi.org/10.15680/IJRSET.2016.0505268>
4. Rani B. J., Ravina M., Saravanakumar B., Ravi G., Ganesh V., Ravichandran S., Yuvakkumar R. Ferrimagnetism in cobalt ferrite (CoFe_2O_4) nanoparticles. *Nano-Structures & Nano-Objects*. 2018;14: 84–91. <https://doi.org/10.1016/j.nanoso.2018.01.012>
 5. Manouchehri S., Ghasemian Z., Shahbazi-Gahrouei D., Abdollah M. Synthesis and characterization of cobalt-zinc ferrite nanoparticles coated with DMSA. *Chem Xpress*. 2013;2(3):147–152. <https://www.tsijournals.com/articles/synthesis-and-characterization-of-cobaltzinc-ferritenanoparticles-coated-with-dmsa.pdf>
 6. Lopez. P. P. J., Gonzalez - Bahamon L. F., Prado J., Caicedo J. C., Zambrano G., Gomez M. E., Esteve J. Study of magnetic and structural properties of ferrofluids based on cobalt-zinc ferrite nanoparticles. *Journal of Magnetism and Magnetic Materials*. 2012;324(4): 394–402. <https://doi.org/10.17586/2220-8054-2016-7-4-624-628>
 7. Singhal S., Namgyal T., Bansal S., Chandra K. Effect of Zn substitution on the magnetic properties of cobalt ferrite nano particles prepared via sol-gel route. *Journal of Electromagnetic Analysis and Applications*. 2010;2(6): 376–381. <http://dx.doi.org/10.4236/jemaa.2010.26049>
 8. Gaikwad R. S., Chae S.-Y., Mane R. S., Han S.-H., Joo O.-S. Cobalt ferrite nanocrystallites for sustainable hydrogen production application. *International Journal of Electrochemistry*. 2011: 1–6. <https://doi.org/10.4061/2011/729141>
 9. Ladole C. A. Preparation and characterization of spinel zinc ferrite ZnFe_2O_4 . *International Journal of Chemical Science*. 2012;10(3): 12301234. <https://www.tsijournals.com/articles/preparation-and-characterization-of-spinel-zinc-ferrite-znfe2o4.pdf>
 10. Raghuvanshi S., Kane S. N., Tatarchuk T. R., Mazaleyrat F. Effect of Zn addition on structural, magnetic properties, antistructural modeling of $\text{Co}_{1-x}\text{Zn}_x\text{Fe}_2\text{O}_4$ nano ferrite. *AIP Conference Proceedings* 1953. 2018: 030055. <https://doi.org/10.1063/1.5032390>
 11. Sawadzky G. A., Van der Woude F., Morrish A. H. Cation distributions in octahedral and tetrahedral sites of the ferrimagnetic spinel CoFe_2O_4 . *Journal of Applied Physics*. 1968;39(2): 1204–1206. <https://doi.org/10.1063/1.1656224>
 12. Haiduk Yu. S., Korobko E. V., Shevtsova K.A., Kotikov D. A., Svito I.A., Usenka A. E., Ivashenko D. V., Fakhmi A., Pankov V. V. Synthesis, structure and magnetic properties of cobalt-zinc nanoferrite for magnetorheological liquids. *Kondensirovannye sredy i mezhfaznye granitsy = Condensed Matter and Interphases*. 2020;22(1): 28–38. <https://doi.org/10.17308/kcmf.2020.22/2526>
 13. Chinnasamy C. N., Jeyadevan B., Shinoda K., Tohji K., Djayaprawira D. J., Takahashi M., Joseyphus R. J., Narayanasamy A. Unusually high coercivity and critical single-domain size of nearly monodispersed CoFe_2O_4 nanoparticles. *Applied Physics Letters*. 2003;83(14): 2862–2864. <https://doi.org/10.1063/1.1616655>
 14. Lin Q., Xu J., Yang F., Lin J., Yang H., He Y. Magnetic and mössbauer spectroscopy studies of zinc-substituted cobalt ferrites prepared by the sol-gel method. *Materials*. 2018;11(10): 1799. <https://doi.org/10.3390/ma11101799>
 15. Liu Y., Zhu X. G., Zhang L., Min F. F., Zhang M. X. Microstructure and magnetic properties of nanocrystalline $\text{Co}_{1-x}\text{Zn}_x\text{Fe}_2\text{O}_4$ ferrites. *Materials Research Bulletin*. 2012;47: 4174–4180. <https://doi.org/10.1016/j.materresbull.2012.08.076>
 16. Ranjani M., Jesurani S., Priyadharshini M., Vennila S. Sol-gel synthesis and characterization of zinc substituted cobalt ferrite magnetic nanoparticles. *International Journal of Advanced Research*. 2016;5(6): 882–886. <https://doi.org/10.17577/IJERTV5IS060665>
 17. Copolla P., da Silva F. G., Gomide G., Paula F. L.O., Campos A.F. C., Perzynski R., Kern C., Depeyrot G., Aquino R. Hydrothermal synthesis of mixed zinc-cobalt ferrite nanoparticles: structural and magnetic properties. *Journal of Nanoparticle Research*. 2016;18(138): 1–15. <https://doi.org/10.1007/s11051-016-3430-1>
 18. Praveena K., Sadhana K. Ferromagnetic properties of Zn substituted spinel ferrites for high frequency applications. *International Journal of Scientific and Research Publications*. 2015;5(4): 121. Available at: <http://www.ijsrp.org/research-paper-0415.php?rp=P403877>
 19. Komogortsev S. V., Patrusheva T.N., Balaev D. A., Denisova E. A., Ponomarenko I. V. Cobalt ferrite nanoparticles based on mesoporous silicon dioxide. *Pis'ma v Zhurnal teoreticheskoi fiziki*. 2009;35(19): 6–11. (In Russ.). <https://www.elibrary.ru/item.asp?id=20326999>
 20. Komogortsev S. V., Iskhakov R. S., Balaev A. D., Kudashov A. G., Okotrub A. V., Smirnov S. I. Magnetic properties of Fe_3C ferromagnetic nanoparticles encapsulated in carbon nanotubes *Physics of the Solid State*. 2007;49(4): 734–738. <https://doi.org/10.1134/s1063783407040233>

Information about the authors

Yulyan S. Haiduk, PhD in Chemistry, Senior Researcher, Belarusian State University (Minsk, Belarus).

<https://orcid.org/0000-0003-2737-0434>

j_haiduk@bk.ru

Evguenia V. Korobko, DSc in Technical Sciences, Professor, Head of Laboratory, A. V. Luikov Heat and Mass Transfer Institute of the National Academy of Sciences of Belarus (Minsk, Belarus).

<https://orcid.org/0000-0002-2870-9658>

evkorobko@gmail.com

Dzmitry A. Kotsikau, PhD in Chemistry, Associate Professor, Belarusian State University (Minsk, Belarus).

<https://orcid.org/0000-0002-3318-7620>

kotsikau@bsu.by

Ivan A. Svito, PhD in Physics and Mathematics, Senior Researcher, Belarusian State University (Minsk, Belarus).

<https://orcid.org/0000-0002-4510-0190>

ivansvito184@gmail.com

Alexandra E. Usenka, PhD in Chemistry, Associate Professor, Department of Physical Chemistry, Belarusian State University (Minsk, Belarus).

<https://orcid.org/0000-0002-2251-6193>

usenka@bsu.by

Vladimir V. Pankov, DSc in Chemistry, Professor, Head of the Department of Physical Chemistry, Belarusian State University (Minsk, Belarus).

<https://orcid.org/0000-0001-5478-0194>

pankov@bsu.by

Received September 9, 2021; approved after reviewing October 1, 2021; accepted for publication December 15, 2021; published online March 25, 2022.

Translated by Yulia Dymant

Edited and proofread by Simon Cox